PRIFYSGOL ABERYSTWYTH UNIVERSITY

Aberystwyth University

Automatic Estimation of Wheat Grain Morphometry from CT Data

Strange, Harry; Zwiggelaar, Reyer; Sturrock, Craig; Mooney, Sacha; Doonan, John

Published in:
Functional Plant Biology

DOI:
10.1071/FP14068

Publication date:
2015

Citation for published version (APA):
Strange, H., Zwiggelaar, R., Sturrock, C., Mooney, S., & Doonan, J. (2015). Automatic Estimation of Wheat Grain Morphometry from CT Data. *Functional Plant Biology*, *42*, 452-459. https://doi.org/10.1071/FP14068

General rights
Copyright and moral rights for the publications made accessible in the Aberystwyth Research Portal (the Institutional Repository) are retained by the authors and/or other copyright owners and it is a condition of accessing publications that users recognise and abide by the legal requirements associated with these rights.

• Users may download and print one copy of any publication from the Aberystwyth Research Portal for the purpose of private study or research.
• You may not further distribute the material or use it for any profit-making activity or commercial gain
• You may freely distribute the URL identifying the publication in the Aberystwyth Research Portal

Take down policy
If you believe that this document breaches copyright please contact us providing details, and we will remove access to the work immediately and investigate your claim.

tel: +44 1970 62 2400
email: is@aber.ac.uk

Download date: 02. Mar. 2024

CSIRO PUBLISHING
Functional Plant Biology
http://dx.doi.org/10.1071/FP14068

Automatic estimation of wheat grain morphometry from computed tomography data

Harry Strange[A,D], *Reyer Zwiggelaar*[A], *Craig Sturrock*[B], *Sacha J. Mooney*[B] *and John H. Doonan*[C]

[A]Department of Computer Science, Aberystwyth University, Aberystwyth, SY23 3DB, UK.
[B]School of Biosciences, University of Nottingham, Sutton Bonnington, LE12 5RD, UK.
[C]National Plant Phenomics Center, Institute of Biological, Environmental and Rural Sciences, Aberystwyth University, Aberystwyth, SY23 3EB, UK.
[D]Corresponding author. Email: hgs08@aber.ac.uk

Abstract. Wheat (*Triticum aestivum* L.) grain size and morphology are playing an increasingly important role as agronomic traits. Whole spikes from two disparate strains, the commercial type Capelle and the landrace Indian Shot Wheat, were imaged using a commercial computed tomography system. Volumetric information was obtained using a standard back-propagation approach. To extract individual grains within the spikes, we used an image processing pipeline that included adaptive thresholding, morphological filtering, persistence aspects and volumetric reconstruction. This is a fully automated, data-driven pipeline. Subsequently, we extracted several morphometric measures from the individual grains. Taking the location and morphology of the grains into account, we show distinct differences between the commercial and landrace types. For example, average volume is significantly greater for the commercial type ($P = 0.0024$), as is the crease depth ($P = 1.61 \times 10^{-5}$). This pilot study shows that the fully automated approach described can retain developmental information and reveal new morphology information at an individual grain level.

Additional keywords: grain analysis morphometric measurements, segmentation.

Received 28 February 2014, accepted 12 August 2014, published online 5 November 2014

Introduction

The domestication of wheat (*Triticum aestivum* L.) is believed to have occurred around 10 000 years ago and coincided with a major cultural transition in human society. The increased and changed diet, facilitated by wheat and other domesticated cereals, has had ongoing effects on human health, evolution and population size. Wheat currently provides about one-fifth of the calories consumed by humans (Dubcovsky and Dvorak 2007) and is economically one of Europe's key crop species. One of the characteristics that distinguishes domesticated breadwheat from its wild ancestors is an increase in grain size (Fuller 2007; Brown *et al.* 2009) and a change in shape (Gegas *et al.* 2010). Partly because of its effect on yield, increasing grain size continues to be a major selection and breeding target in modern wheat (Kovach *et al.* 2007). Shape has been a relatively recent breeding target dictated by the market and industry requirements. Indeed, grain shape (and size), density and uniformity are important attributes for determining the market value of wheat grain, since they influence the milling performance (i.e. flour quality and yield). It has been proposed that milling yield could be increased by optimising grain shape and size, and modelling indicates that large and spherical grains would provide the optimum grain morphology (Evers *et al.* 1990).

Characteristics such as grain weight, dimensions and uniformity, contribute indirectly to the industry standard test weight (grain weight per volume). The complex nature of these traits, however, makes improvements difficult. Nevertheless, several quantitative trait loci and genes associated with seed morphology have been identified in wheat, barley (*Hordeum vulgare* L.) and rice (*Oryza sativa* L.). The nature of the genes underlying any of the quantitative trait loci identified and the precise means by which grain size and shape differ between existing germplasm, however, are not known. Methods available for quantitative analysis of cereal grain variation usually depend on bulk physical parameters, such as thousand grain weight (Groos *et al.* 2003) or bulk packing density (Doehlert *et al.* 2006; Wychowaniec *et al.* 2013). Other methods, usually based on computer vision, provide data on individual grains and can yield insight into the within-sample variation in grain shape and size (Gegas *et al.* 2010). However, most of these methods use loose mature grain, so potentially valuable developmental information is lost and the more complex aspects of grain shape (e.g. the crease, (Sun *et al.* 2007)) are rarely considered.

Kernel number per spike is a key agronomic trait that has a major impact on yield. However, it is complex and includes

Journal compilation © CSIRO 2014

component traits such spike length, spikelet number per spike, fertile spikelet number, sterile spikelet number and compactness (Ma *et al.* 2007), and many of these traits seem to be differentially regulated during the development of the spike. Analysis of bulk grain often fails to capture variation in such traits and manual dissection of the spike, though very effective, is laborious. Methods that allow automated capture and analysis of spike- and grain-related traits could therefore be of immense use in plant biology and breeding.

The reduced cost and increased availability of X-ray computed tomography (CT) scanners provides a possible approach to overcome these barriers. In this paper, we describe a simple method based on CT scanning and reconstruction that captures grain shape *in situ*, allowing one to relate grain shape and size to developmental position on the spike, as well as to compare between strains. This nondestructive method is relatively rapid and could be scaled to a larger sample size. Additional computer-vision techniques (such as volumetric visualisation and registration) could be used to extract additional parameters and structures from the images. We use it to compare two disparate types of wheat, an elite commercial type and a traditional landrace type, with different spike morphologies and grain types. The approach quantitatively captures the developmental-related variation in grain shape along the spike and provides a comparison between the types, in addition to revealing quantitative differences in crease morphology.

The novelty of this work is therefore twofold. First, to the best of our knowledge, we present the first ever work on automatic segmentation and morphometric analysis of wheat CT data. Second, we present a simple segmentation procedure for automatically identifying wheat grain from such CT scans that is easy to replicate.

Materials and methods

Plant material and imaging conditions

Two disparate strains of wheat (*Triticum aestivum* L.), the commercial type Capelle and the landrace Indian Shot Wheat, were grown to maturity in field plots and allowed to ripen. Whole spikes harvested intact, taking care to avoid grain loss. Fig. 1 shows the resulting segmentations of the two strains found using the proposed approach and Fig. 2 illustrates the terms used when describing the botany of the wheat plant.

X-ray CT scans were acquired using a Phoenix Nanotom 180NF scanner (GE Sensing and Inspection Technologies, Wunstorf, Germany) in 'multiscan mode' at a maximum electron acceleration energy of 65 kV and a current of 140 µA. The samples were wrapped in a thin low-density polystyrene sheet and then placed in a plastic test tube to minimise movement during the scan. In total, 1200 projection images were collected over a 360° rotation of the sample with the detector in 2×2 binning mode (1152×1152 pixels), a 750-ms exposure time and three-image averaging. The time for the multiscan was 80 min and the spatial resolution was 54 µm. 'Multiscan mode' consists of the combination of reconstructed volumes of two (or more) individual scans (top and bottom of the sample in the *y*-axis) to maximise the spatial resolution while capturing the entire length of the wheat spike. Image slice data was outputted in 16-bit tagged image file format.

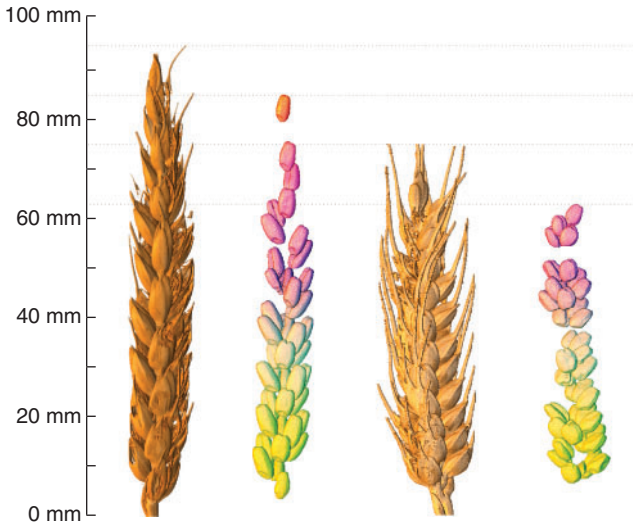

Fig. 1. Example segmentations taken from computed tomography scans of commercial breadwheat (left) and Indian Shot Wheat (right) obtained using the approach outlined in Figs 4 and 5.

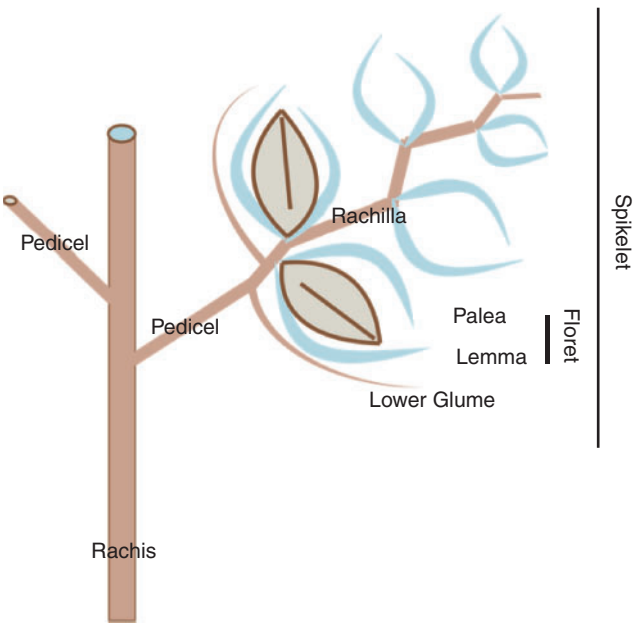

Fig. 2. Illustration of a wheat spike modified from Kirby and Appleyard (1987) (courtesy of Arable Unit RASE).

Ground truth estimation

To evaluate the performance of the proposed grain segmentation algorithm, a set of ground truth segmentations was produced that delineated grain from the background in certain scan slices. A set of 20 slices was selected from the scans at random, 10 from the scans of Indian Shot Wheat and 10 from the commercial bread wheat. Three users then provided ground

truth segmentations for each of these slices using the freely available LabelMe tool (http://labelme.csail.mit.edu, accessed 6 October 2014; Russell *et al.* 2008). An example of a slice showing ground truth segmentations is shown in Fig. 3. This resulted in a set of binary masks representing the grain regions on each of these 20 slices. A majority voting scheme was used to combine the different users' segmentations and so determine the final ground truth segmentation for each slice.

Grain segmentation

The grain was segmented from the CT volume using a multistep segmentation process. Initially, the slices within the volume were thresholded using an adaptive histogram thresholding method. Small, noisy regions were then removed using morphological filtering. Subsequently, a persistence approach was used to filter the grain from any remaining floral organ structures. The final step was to smooth each of the identified wheat grains using morphological processing.

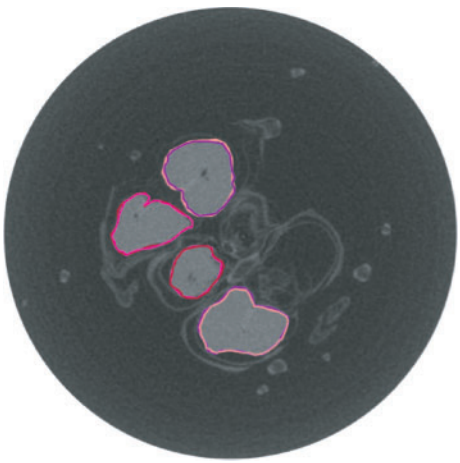

Fig. 3. Ground truth segmentations overlaid on a slice through the Indian Shot Wheat scan. Different colours correspond to different users' segmentations obtained using the LabelMe tool (Russell *et al.* 2008).

The first step was to segment the wheat grain from any background region using an adaptive thresholding approach. Thresholding seeks to separate an image into two distinct regions (foreground and background) by assigning all pixels whose intensity value is less than the given threshold into the background region, and all pixels whose intensity is greater than the given threshold into the foreground region. A single-user defined threshold did not suffice in this application, since differing imaging conditions meant that the wheat grain appeared with different intensities across CT scans. Therefore, the threshold was automatically learnt for each CT volume by examining the distribution of intensities over the entire volume. The distribution was bimodal (Fig. 4), with the major mode corresponding to the background and noisy regions and the minor mode corresponding to areas of wheat grain. This bimodal distribution can be thought of a mixture of two Gaussians with the means corresponding to the two modes. The threshold can then be learnt by setting the threshold value to the mean of the Gaussian corresponding to the minor mode minus half the width of the Gaussian (Fig. 4).

The task therefore becomes to extract the smaller of the two Gaussians. This was done by performing peak detection on the entire histogram of the distributions. Peaks appeared as local maxima on the histogram and so the two most prominent peaks was extracted, the smaller of which correspondedto the mean (μ) of the Gaussian we wish to model. Having found the mean, the s.d. is then directly learnt from the histogram. The threshold was then set as $t = \mu - w$, where w is the full width at one-tenth of the maximum. Fig. 4 shows this process along with a sample segmentation obtained using the adaptive thresholding approach.

As can been seen from Fig. 4*b*, although the wheat grains were segmented using the approach described above, some smaller noisy regions were also present in the segmentation. Therefore, a two-stage filtering methodology was used to remove any noisy regions and segment only the wheat grain regions. First, any regions (connected components) with fewer than 25 pixels were removed and the regions were eroded using a morphological erosion operation (Soille 2004) with a three-pixel disk structuring

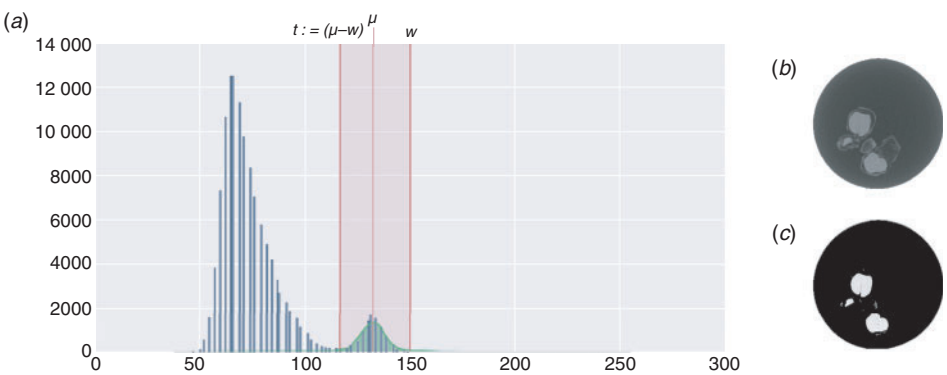

Fig. 4. (*a*) A histogram of pixel intensities over an entire computed tomography (CT) volume. The histogram is bimodal in nature and can be modelled as a mixture of two Gaussians, the smaller of which corresponds to wheat grain pixels. A threshold to segment wheat grain from the background can be learnt from this Gaussian by setting the threshold as the mean of the Gaussian (μ) minus the half width (i.e. $t := \mu - w$). (*b*) A slice from this CT volume. (*c*) The same slice segmented using the automatically learnt threshold.

element to separate any touching regions. Second, a persistence approach was employed, whereby only regions with long lifespans through the volume were kept.

To perform persistence based filtering, the lifespan of each connected component within the thresholded volume was recorded. The lifespan of a connected component is the number of slices that the connected component appears in. The basic intuition of persistence-based filtering is that the wheat grain will have a longer lifespan and thus persist over the volume, whereas smaller noisy regions will have a shorter lifespan and can therefore be ignored. Once the lifespans of all the connected components were measured, they were sorted in ascending order. The largest 'jump' between two consecutive lifespans as then taken to be the threshold that distinguished wheat grain from nongrain regions (Fig. 5). Any connected component whose lifespan was larger than this jump was retained and corresponded to the extracted wheat grain regions.

The final stage of the segmentation process was to refine the segmented regions using morphological filtering. Morphological dilation (Soille 2004) is performed with a disk-based structuring element of radius 3, which counteracted the erosion mentioned above. Each connected component was then smoothed using a $3 \times 3 \times 3$ Gaussian kernel and the final binary segmentations were produced by performing Otsu's thresholding method on each slice (Otsu 1979).

Fig. 6 shows a set of slices through different CT volumes with the results of the above segmentation process overlaid. Figs 7 and 8 show 3D reconstructions of two different types of wheat grain segmented from CT scans using this approach.

Extraction of morphometric measures

Measures were taken from each of the 3D connected components (corresponding to individual wheat grain) after segmentation had been performed. The morphometric measures that were automatically extracted were length, width, length width ratio, volume, crease depth ratio and hole volume. Fig. 9 shows the key measures extracted from the wheat grain from which the abovementioned morphometric measures were derived. The length and width were measured as the first and second major axes of the ellipsoid fitted around the middle slice of the connected component respectively. The length : width ratio was then taken to be the length divided by the width and corresponds to the horizontal axis proportion. The volume corresponded to the total number of pixels segmented per connected component.

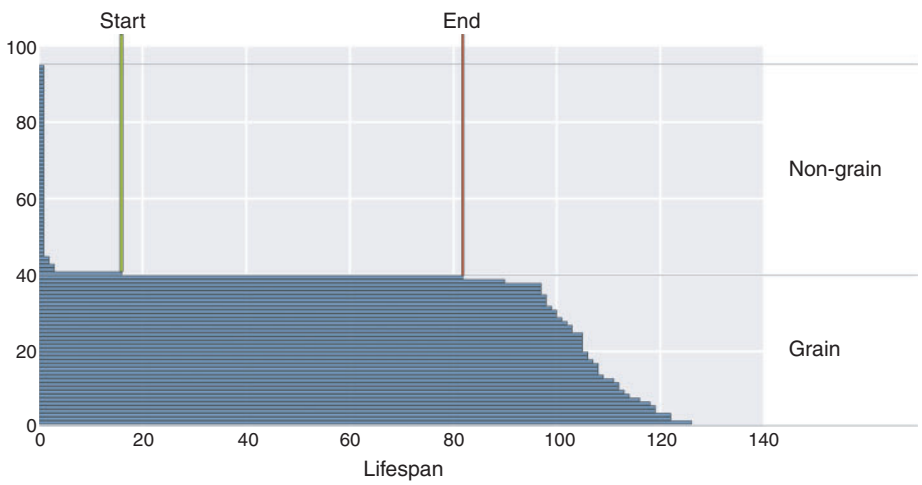

Fig. 5. The lifespan of all connected components measured throughout the volume of the computed tomography scan sorted in ascending order. There is a noticeable 'jump' corresponding to the difference between noisy regions and regions corresponding to wheat grains. The start and end point of this jump are highlight by the green and red marker respectively. This 'jump' was used to filter grain from nongrain during the segmentation process.

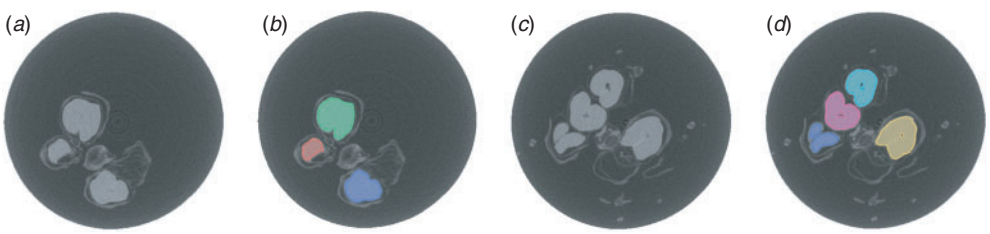

Fig. 6. Cross-sections of wheat computed tomography volumes (*a*, *c*) along with the resulting segmentations acquired (*b*, *d*). Both cross-sections (*a*, *c*) are taken from Indian shot wheat scans.

The crease depth was calculated by examining the middle slice of each connected component. A convex hull was taken around the segmentation of the middle slice that encompassed the segmented wheat grain area as well as the crease area. The difference between the convex hull and the segmentation revealed the crease area. The height of this crease area then corresponded to the crease depth.

The hole volume was used to examine whether there were any voids within the wheat grain. The hole volume was measured as the total volume of any voids found within the wheat grain (Fig. 9). The voids were found by finding any pixels within the segmented wheat grain that were labelled as 0 in the segmentation mask. These pixels corresponded to voids within the segmentation and therefore voids within the wheat grain.

Results

Although CT scanning can provide very accurate measurements of overall spike size (Fig. 1), its main attraction in this application was the ability to reveal the complex structure of the spike. The spike is composed of a central rachis that bears branches called spikelets. The wheat spikelet meristem is indeterminate and can generate up to 12 floret primordia. At most, only four or five of these primordia produce functional florets (Langer and Hanif 1973) and usually only two or three filled grains are produced. The number of filled grains per spikelet and their quality, for example, are important agronomic traits that would be scored by manual dissection.

Segmentation of the grains from the spike material provides a novel imaging method that retains the location and orientation of the grains relative to the floral organs within the spike (Fig. 1). Closer inspection of the spikes revealed that the grains tended to cluster in groups of three fully filled grains at the base of the spikes. In the mid-zone, the clusters were still comprised of three grains but, often, one of the grains was smaller. At the apex of the spike, the grains were singly spaced (McMaster 1997).

The segmentations produced in this manner closely matched those of the ground truth. The overall accuracy of the proposed method compared against ground truth was 99.7% (±0.003). Accuracy was measured as the total number of correctly identified pixels divided by the total number of pixels in the image. The proposed method achieved a sensitivity of 0.95

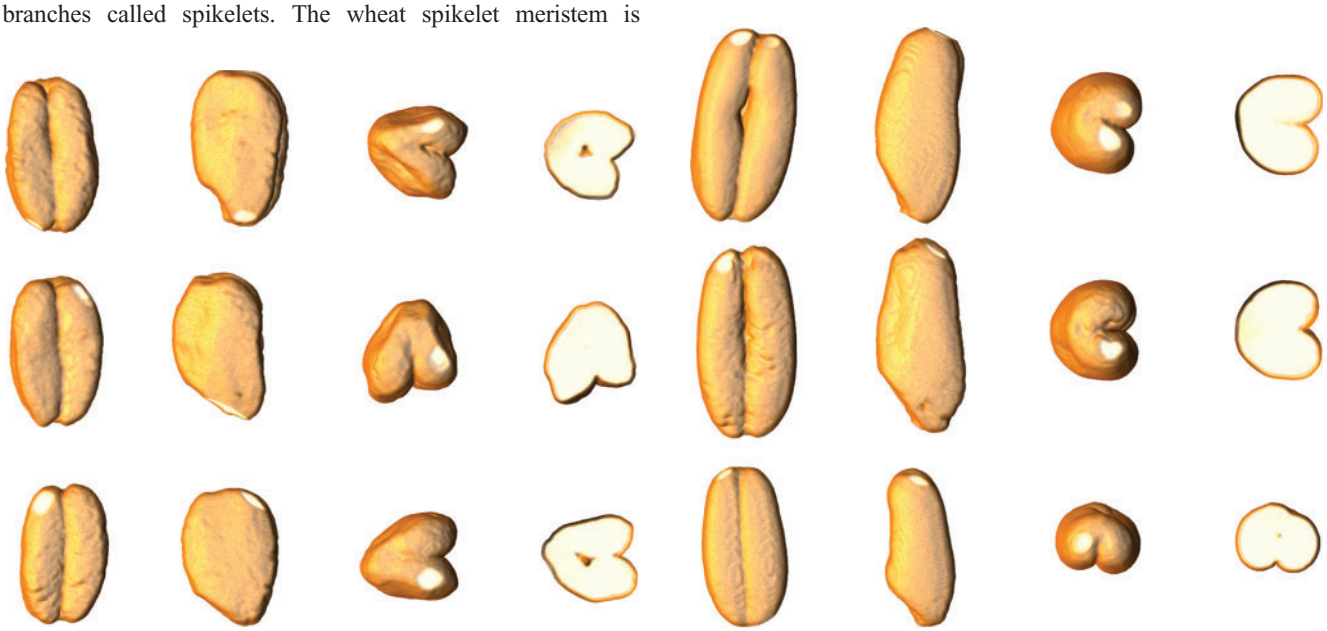

Fig. 7. 3D reconstructions of Indian Shot Wheat grain.

Fig. 8. 3D reconstructions of the commercial breadwheat grain.

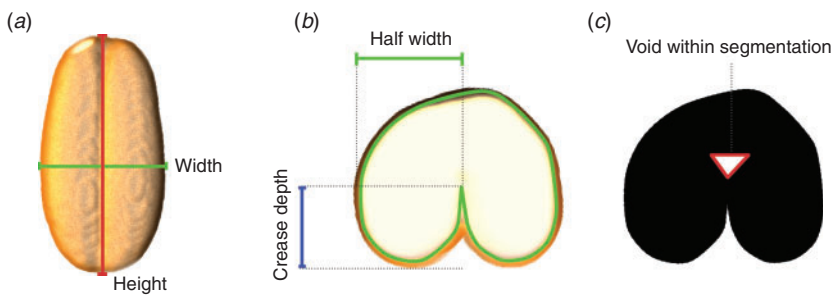

Fig. 9. Examples of the morphometric measures that were automatically extracted from the segmented wheat grain: (*a*) width and height; (*b*) half width and crease depth; (*c*) void within segmentation.

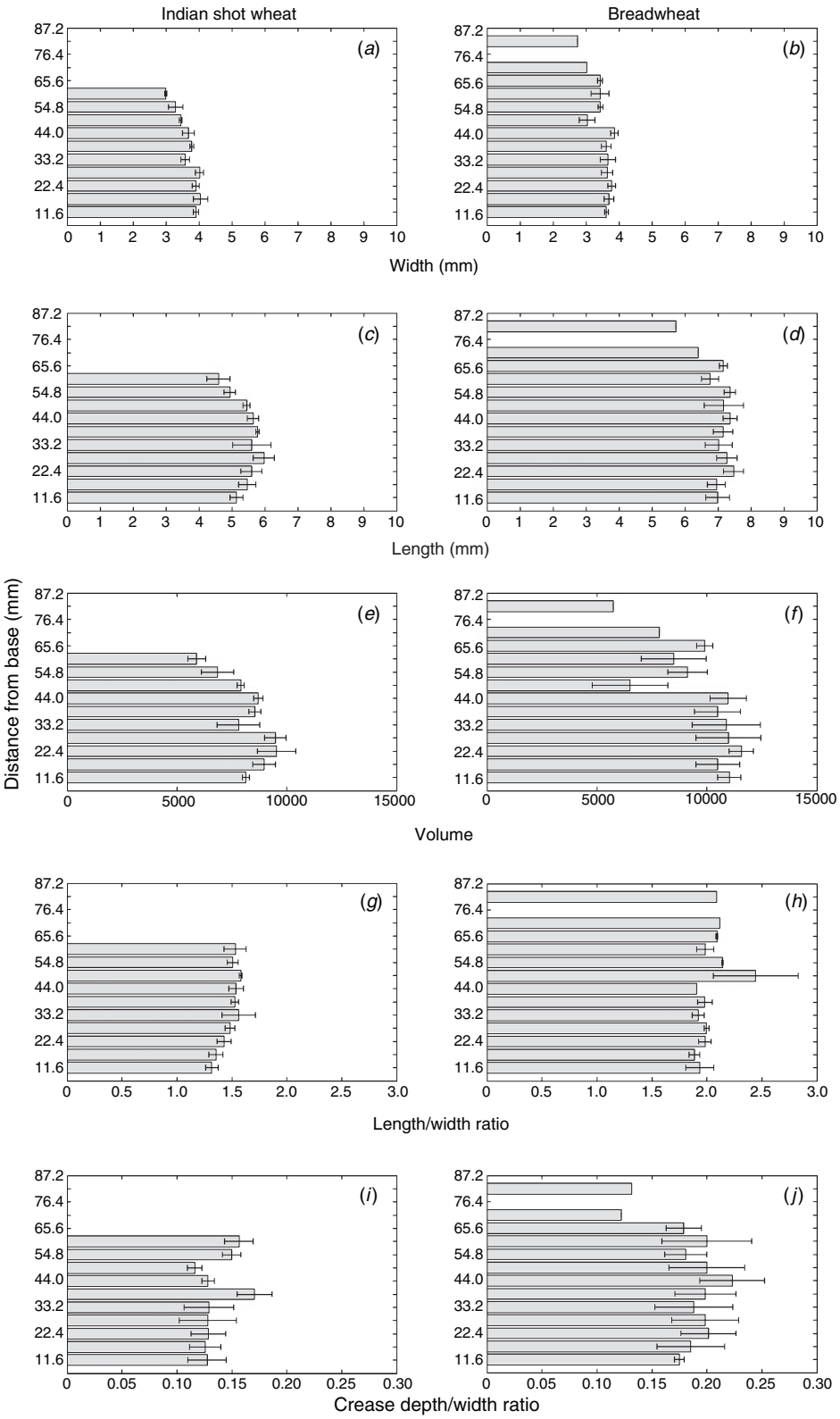

Fig. 10. Comparison of measures for (*a*, *c*, *e*, *g*, *i*) Indian Shot Wheat (left column) and (*b*, *d*, *f*, *h*, *j*) commercial breadwheat (right column). The histograms show the distributions ordered by their distance from the base of the spike. The sample sizes for the Indian shot wheat and commercial breadwheat are $n = 31$ and $n = 39$ respectively. (*a*, *b*) Width; (*c*, *d*) length; (*e*, *f*) volume; (*g*, *h*) length : width ratio; (*i*, *j*) crease depth : width ratio.

(±0.03) and a specificity of 0.99 (±0.00). As well as this, the Dice coefficient (Dice 1945) was used to compare the similarity of the individual grain segmentations to their related ground truth. The Dice coefficient was bounded by 0 and 1, with 0 indicating no similarity and 1 indicating an exact similarity. The overall Dice value of the proposed method was 0.94 (±0.04), indicating a strong similarity between the proposed segmentations and the ground truth.

To evaluate the utility of the approach to acquiring quantitative grain characteristics in their developmental context and from different strains, we compared length, width, volume and crease depth relative to grain position along the rachis (Fig. 10), and between commercial and landrace types (Figs 10 and 11). Grain width showed a slight increase from the base to central region, with a gentle decline towards the apex in the commercial wheat. The shot wheat grain width was greater (average = 3.76 mm as opposed to 3.52 mm) but showed a less even pattern of change along the rachis. The change in grain length followed broadly similar patterns in both strains, with a gentle decline from base to apex, although there was a significant difference ($P = 4.80 \times 10^{-18}$) in average length (5.47 mm *vs* 7.08 mm, Fig. 11). Grain volume was fairly constant near the base of the rachis and then gently declined towards the apex in the commercial wheat, but showed a more irregular pattern in Indian Shot Wheat. Interestingly, the analysis revealed a greater spread of volume in the commercial wheat, although, as expected, the average volume was significantly ($P = 0.0024$) greater (Fig. 11). The length : width ratio was closer to 1 in the landrace type (1.46), reflecting its name 'Indian Shot Wheat', as opposed to 2.03 in the commercial type.

Average crease depth (as measured halfway along the grain) in the commercial type was ~1.5 times that of Indian Shot Wheat (Fig. 11). The crease depth followed a similar trend to width in both strains, except at the apex, where the crease depth increased in both strains (Fig. 10). Again, there was a significant difference between the strains when comparing crease depth ($P = 1.61 \times 10^{-5}$).

The crease is a complex and variable morphological feature that varies from a relatively simple 'V' shape to an inverted 'T' or even a 'D' shape (where there is an internal void). A V-shaped crease would provide a hole volume close to zero, whereas other shapes would provide a positive volume. Based on this measure,

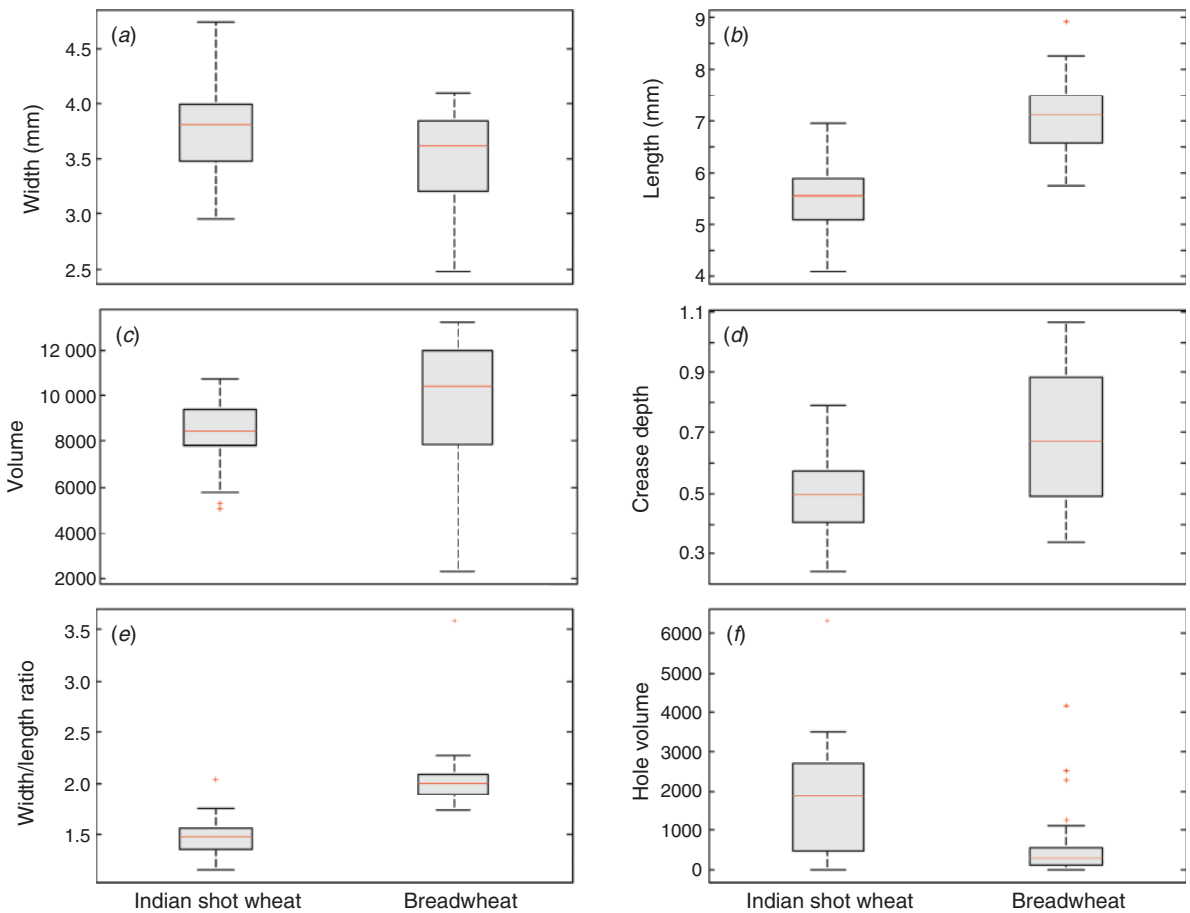

Fig. 11. Boxplot comparisons of the different wheat grain measures taken from Indian Shot Wheat and commercial breadwheat. The boxplots show the distribution of morphometric measures over the entire wheat spike. The *P*-values for each measure are (*a*) width, ($P = 7.90 \times 10^{-3}$; (*b*) length, $P = 4.80 \times 10^{-18}$; (*c*) volume, $P = 2.40 \times 10^{-3}$; (*d*) crease depth, $P = 1.61 \times 10^{-5}$; (*e*) width : length ratio, $P = 1.83 \times 10^{-17}$; (*f*) hole volume, $P = 1.05 \times 10^{-5}$. The sample sizes for the Indian Shot Wheat and commercial breadwheat are $n = 31$ and $n = 39$ respectively.

the two types were dramatically different: the commercial type was close to zero, indicating a V-shaped crease whereas the Indian Shot Wheat had a dramatically increased score that was highly variable.

Discussion and conclusions

In this paper, we demonstrate the utility of CT scanning, image segmentation and reconstruction for capturing grain characteristics that would be very difficult or time-consuming to capture by traditional means. Notably, this method has the potential to retain developmental information that is lost in bulk grain analysis and to reveal new information on grain structure that has, hitherto, only been available by means of manual dissection. The simplicity of the segmentation algorithm makes it easy to implement, fast to run and easily scalable. Further work will examine (a) extending the segmentation approach to automatically identifying and extracting the surrounding floral organs and branching morphology, and (b) scaling the technology to where it can be applied to whole breeding populations. This could be facilitated by the use of a new CT scanner with scan times being reduced from 80 min to 10 min for the whole spike.

Acknowledgements

We thank Biotechnology and Biological Sciences Research Council for funding (BB/J004464/1) as well as the National Institute for Social Care and Health Research Biomedical Research Unit for advanced medical imaging and visualisation. We also thank Jonathan Roscoe, Andrik Rampin and Shiseng Wang for help with providing the ground truth annotations.

References

Brown TA, Jones MK, Powell W, Allaby RG (2009) The complex origins of domesticated crops in the Fertile Crescent. *Trends in Ecology & Evolution* **24**, 103–109. doi:10.1016/j.tree.2008.09.008

Dice LR (1945) Measures of the amount of ecologic association between species. *Ecology* **26**(3), 297–302. doi:10.2307/1932409

Doehlert DC, McMullen MS, Jannink J-L (2006) Oat grain/groat size: a physical basis for test weight. *Cereal Chemistry* **83**(1), 114–118. doi:10.1094/CC-83-0114

Dubcovsky J, Dvorak J (2007) Genome plasticity a key factor in the success of polyploid wheat under domestication. *Science* **316**, 1862–1866. doi:10.1126/science.1143986

Evers AD, Cox RI, Shaheedullah MZ, Withey RP (1990) Predicting milling extraction rate by image analysis of wheat grains. *Aspects of Applied Biology* **25**, 417–426.

Fuller DQ (2007) Contrasting patterns in crop domestication and domestication rates: recent archaeobotanical insights from the Old World. *Annals of Botany* **100**, 903–924. doi:10.1093/aob/mcm048

Gegas VC, Nazari A, Griffiths S, Simmonds J, Fish L, Orford S, Sayers L, Doonan JH, Snape JW (2010) A genetic framework for grain size and shape variation in wheat. *The Plant Cell* **22**(4), 1046–1056. doi:10.1105/tpc.110.074153

Groos C, Robert N, Bervas E, Charmet G (2003) Genetic analysis of grain protein-content, grain yield and thousand-kernel weight in bread wheat. *Theoretical and Applied Genetics* **106**(6), 1032–1040.

Kirby EJM, Appleyard M (1987). 'Cereal development guide.' (NAC Cereal Unit: Stoneleigh, Kenilworth)

Kovach MJ, Sweeney MT, McCouch SR (2007) New insights into the history of rice domestication. *Trends in Genetics* **23**, 578–587. doi:10.1016/j.tig.2007.08.012

Langer RHM, Hanif M (1973) Study of floret development in wheat (*Triticum aestivum* L.). *Annals of Botany* **37**(152), 743–751.

Ma Z, Zhao D, Zhang C, Zhang Z, Xue S, Lin F, Kong Z, Tian D, Luo Q (2007) Molecular genetic analysis of five spike-related traits in wheat using RIL and immortalized F_2 populations. *Molecular Genetics and Genomics* **277**(1), 31–42. doi:10.1007/s00438-006-0166-0

McMaster GS (1997) Phenology, development, and growth of the wheat (*Triticum aestivum* L.) shoot apex: a review. *Advances in Agronomy* **59**, 63–118. doi:10.1016/S0065-2113(08)60053-X

Otsu N (1979) A threshold selection method from gray-level histograms. *IEEE Transactions on Systems, Man, and Cybernetics* **9**(1), 62–66. doi:10.1109/TSMC.1979.4310076

Russell BC, Torralba A, Murphy KP, Freeman WT (2008) LabelMe: a database and web-based tool for image annotation. *International Journal of Computer Vision* **77**(1–3), 157–173. doi:10.1007/s11263-007-0090-8

Soille P (2004) 'Morphological image analysis.' 2nd edn. (Springer-Verlag: Berlin)

Sun J, Huang K, Li W, Wang L, Wang A, Huo J, Chen J, Chen C (2007) Effects of wheat flour fortified with different iron fortificants on iron status and anemia prevalence in iron deficient anemic students in Northern China. *Asia Pacific Journal of Clinical Nutrition* **16**(1), 116–121.

Wychowaniec J, Griffiths I, Mughal A, Gay A (2013) Compaction of cereal grain. *Philosophical Magazine* **93**(31–33), 4151–4158. doi:10.1080/14786435.2013.808771